Journal of Nuclear Materials 390–391 (2009) 136–139

Contents lists available at ScienceDirect

Journal of Nuclear Materials

journal homepage: www.elsevier.com/locate/jnucmat

Molecular dynamics simulations of atomic carbon on tungsten surface

Zhongshi Yang [a], Y.M. Yang [b], G.-H. Lu [c], G.-N. Luo [a,*]

[a] Institute of Plasma Physics, Chinese Academy of Sciences, P.O. Box 1126, Hefei 230031, China
[b] State Key Lab of Mechanical Transmissions, Chongqing University, Chongqing 400044, China
[c] Department of Physics, Beijing University of Aeronautics and Astronautics, Beijing 100083, China

ARTICLE INFO

PACS:
31.15.xv
34.35.+a
52.40.Hf
81.05.Bx

ABSTRACT

By means of molecular dynamics simulations using bond-order potential, we have investigated the behavior of atomic carbon on both bcc tungsten (001) surface, and amorphous tungsten surface that is formed by a simulated annealing process, at finite temperature (T = 300 K) with incident energy ranging from 0.5 eV to 200 eV. The particle and energy reflection coefficients as well as mean range distribution as a function of incident energy at normal incidence have been calculated and the channeling effect in the energy range above 100 eV has also been discussed. The results are compared with those calculated by Eckstein using binary collision (BC) Code TRIM.SP in the energy range from 55 eV to 200 eV.

1. Introduction

Tungsten (W) and its alloys have been considered as candidate plasma-facing materials (PFMs) for ITER [1], future DEMO reactors [2,3] and EAST [4]. As long as both elements, tungsten and carbon, are introduced in the main chamber of a fusion device, mixing with carbon on the tungsten material surface will be unavoidable because carbon based material is easy to be eroded and the carbon atoms will generally migrate to other locations due to long-range plasma transport processes and interact with the tungsten surface [1,5,6]. Therefore, it is necessary to understand and predict the tungsten surface properties and performance in the presence of C impurities.

The existing experimental data were completely limited in the energy range of keV for carbon projectiles interacting with tungsten surface [7–9] and simulations were mainly based on the binary collision approximation and adopted amorphous target materials [7,10]. In the lower incident energy range, which is more important in a fusion device, experimental data are absent. When the mean free path of ions at low incident energies approaches the average atomic spacing in the target, BC model breaks down and many-body nature has a dramatic effect on the interaction between projectiles and target atoms, requiring molecular dynamics (MD) for accurate simulation. In this work, the particle and energy reflection coefficients as well as mean range distributions of incident atomic carbon on tungsten surface have been calculated using classical MD simulations, and an analytical bond-order potential for modeling non-equilibrium processes in the ternary W–C–H system [11]. Due to the scarcity of experimental results, we will compare our simulation results to Eckstein's data in Ref. [12] where gives a collection of sputtering, reflection and range values calculated by a Monte Carlo (MC) program TRIM.SP [13] in the energy range from 55 eV to 40,000 eV at normal incidence.

2. Simulation method

The initial computational cell with the tungsten (001) plane normal to the incidence direction, had a dimension of 63.31 Å × 63.31 Å × 31.65 Å, consisting of 8000 atoms in 20 conventional bcc unit cells in three Cartesian directions. Periodic boundary conditions were imposed in the x- and y-directions in the cell. To form a surface, non-periodic boundary conditions were applied in the z-direction and the atoms in the lowest three atomic layers were kept fixed at their original positions all times. Temperature was controlled using velocity scaling method for the atoms in the three atomic layers both above the fixed layers and at the four side walls. Other tungsten atoms and incident carbon atoms were excluded from temperature control. The analytical bond-order potential [11] was used to describe the W–W and W–C interactions and the cut-off distance was chosen to be 1 nm for all atoms. Each MD step represented 0.1 fs. This value has been chosen in order to obtain total energy conservation even in the case of high-energy impacts.

Atomic carbon projectiles with a series of kinetic energies from 0.5 eV to 200 eV were used in this study. The projectiles were placed at 4 Å above the top surface atoms in z-direction, greater than the potential cut-off radius of 3.0 Å, and the initial x- and y-coordinates were randomly selected within no temperature

* Corresponding author.
E-mail addresses: zsyang@ipp.ac.cn (Z. Yang), gnluo@ipp.ac.cn (G.-N. Luo).

0022-3115/$ - see front matter © 2009 Elsevier B.V. All rights reserved.
doi:10.1016/j.jnucmat.2009.01.146

control area above the cell. Once an incident carbon atom was projected onto the tungsten (001) surface, the MD simulation was performed until thermal equilibrium was reached after the incident atom was backscattered far from the surface or stuck on the surface. Then the next projectile in the same z-position but with random x- and y-coordinates was shot for the next run. Overall 200 runs were performed for a given incident energy.

We also used a simulated annealing process to prepare an amorphous tungsten cell. The initial structure was a random cell consisting of 8000 W atoms, corresponding to a density of 19.25 g/cm^3. Periodic boundary conditions were applied along the three directions. Each MD step represented 1 fs. The system was first heated to 4000 K. Once molten, the sample was equilibrated at 4000 K for 200 ps. The liquid sample was then cooled to 300 K with a linear cooling rate of 40 K ps^{-1}. Finally, the system was equilibrated at 300 K for an additional 50 ps to anneal away any transient structures.

The W–W pair distribution function $g(r)$ for the simulated amorphous cell is shown in Fig. 1 in comparison with the crystalline sample. Typical characteristic of the amorphous structure can be seen from Fig. 1. The first-neighbor peak is corresponding to the first-neighbor peak in the crystalline tungsten cell indicating the short-range order in the amorphous cell. The second peak shifts along the distance and more high-order peaks become broader and less well defined with increasing distance meaning the absence of long-range order.

3. Results and discussion

By using MD simulations, the particle reflection coefficient of carbon atoms was calculated for normal incidence on tungsten surface. Fig. 2(a) shows the calculated results in this work. Two types of surfaces were adopted: bcc tungsten (001) surface and amorphous tungsten surface. In addition, the results calculated by Eckstein [12] are also displayed. A particle reflection of unity means that 100% of particles incident on a surface are reflected. At 10 eV incident energy, the reflection coefficient has a largest value near to unity. When the incident energy is above 10 eV, the reflection coefficient decreases monotonically with increasing incident energy because the energetic projectile has larger probability to be implanted into the tungsten bulk. In this work, the largest incident energy is 200 eV. Compared to Eckstein's results, the MD results in our simulations are systematically higher within the same energy range. The difference may be attributed to the inherent limitations of TRIM which is based on a randomized target structure and the binary collision approximation irrespective of the many-body nature of carbon–tungsten interactions in the low energy range. In Ref. [12], the lowest energy adopted is 55 eV. Below this energy, there are neither experimental results nor any simulation results to date. Using MD simulations in this work, the reflection coefficient and mean range can also be calculated in the energy range below 55 eV. We found that below 10 eV, the reflection coefficient decreases with the decrease in the incident energy and the projectiles have a larger probability to stick on the tungsten surface.

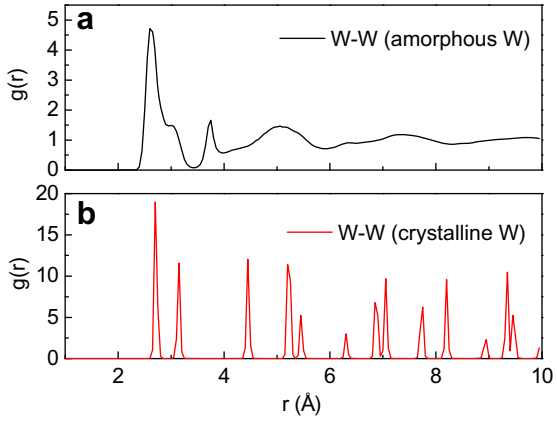

Fig. 1. Tungsten–tungsten pair distribution functions for: (a) the as-created amorphous cell, and (b) bcc crystalline tungsten.

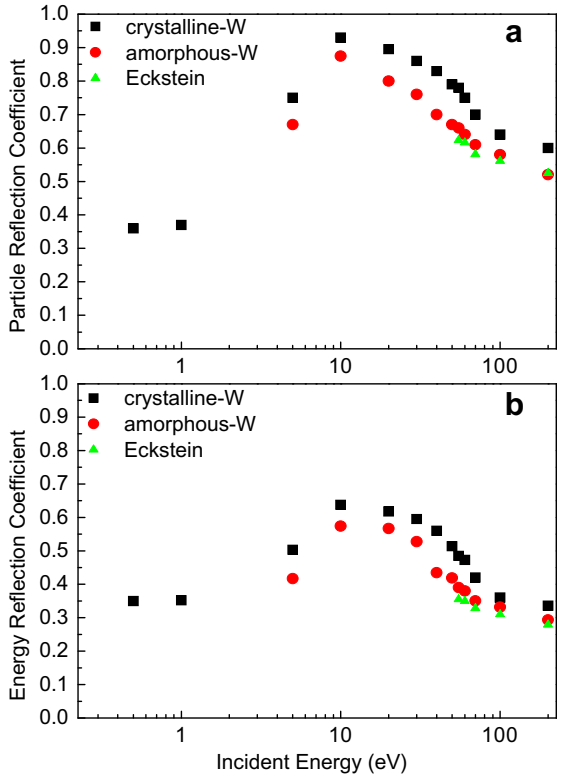

Fig. 2. (a) Particle, and (b) energy reflection coefficients of normal incident carbon atoms on two types of tungsten surfaces, bcc tungsten (001) surface and amorphous tungsten surface, as a function of incident energy. Eckstein's results [12] calculated by TRIM.SP are also displayed. The statistical uncertainties are covered by the graphical markers.

In TRIM simulations, amorphous structure is adopted instead of crystalline one. For comparison, we also calculated the particle reflection coefficient on amorphous tungsten surface in the range of 5–200 eV at normal incidence. Similar to the crystalline cell, the particle reflection coefficient reaches a maximum near 10 eV and decreases monotonically with increasing the incident energy. The values are systematically lower by a factor between 6% and 16% than for the crystalline cell. It is worth noting that in the energy range of 55–200 eV, the results for the amorphous cell are more close to Eckstein's. This means that the surface structure has a pronounced effect on the projectiles' back-scattering behavior. Two types of reflection processes have been observed in this work: (1) direct reflection for the projectiles directly back-scattered after interacting with only a few atoms in the first or second layer; (2) delayed reflection for the projectiles with relatively high kinetic energies that penetrate deep into the bulk, and still flee to the surface, following a temporary residence time [14]. As for the amorphous cell, the random network may act as a labyrinth for the projectiles intruding into it. Following the real-space trajectories of the carbon atoms in delayed reflections, the residence time in the amorphous cell is longer than in the crystalline one, and also, the projectiles in the amorphous structure have much high probability to be trapped.

Also shown in Fig. 2(b) are energy reflection coefficients of the carbon atoms on both of the crystalline and amorphous tungsten surfaces at normal incidence. For comparison, the results calculated by Eckstein are also presented. Energy reflection coefficient is defined as the ratio of reflected energy to total energy incident on the surface. As shown in Fig. 2(b), the energy reflection upon incident energy has a similar trend to the particle reflection. An interesting feature is that in our simulations in low energy range from 0.5 eV to 1 eV, the energy reflection coefficient is very close to the particle reflection coefficient, which means that the scattered particles almost do not lose the kinetic energy after reflection. From the reflected energy distribution for 0.5 eV and 1 eV carbon atoms incident on tungsten surface, we also found that the reflected particles may have energy slightly higher than the incident energy attributed perhaps to the lattice phonon absorption [14].

Fig. 3 shows the average depth (mean range) of the atomic carbons implanted into the crystalline tungsten at normal incidence on (001) tungsten surface with different incident energy. Also shown are the results calculated by adopting the simulated amorphous cell and by Eckstein using TRIM.SP code. The mean projected range represents the most probable location for ion to come to rest. The mean ranges for both crystalline and amorphous surfaces using MD simulations are systematically lower than the results calculated by Eckstein. In low energy range below 10 eV, the un-scattered carbon atoms are absorbed on the top surface layer and cannot penetrate into the bulk, which needs further investigation. With increasing the incident energy above 10 eV, the mean range increases as well as the range straggling. Around the energy of 50 eV, the mean range for the crystalline surface exceeds the result for the amorphous surface which may be attributed to the channeling effect.

In the range of relatively high incident energy of 50–200 eV, we have found the channeling occurs along the ⟨001⟩ crystallographic axis. To analyze the effect, the normal incident carbon atoms were initially placed above the bridge site of tungsten atoms on the top layer. Fig. 4 shows the trajectory of a carbon atom at E_{in} = 150 eV in the tungsten bulk. It can reach the 24th layer below the surface and in the end come to rest in the bulk. Fig. 5 shows the time dependence of the kinetic energy of the channeled carbon atom in Fig. 4 as well as the projected range in tungsten bulk. Before 50 fs, the atom does not make close-impact collisions with lattice atoms and has a very low rate of kinetic energy loss, dE/dx, and slight vibration with small amplitude. When the ion penetrates beyond 20th atomic layers after 50 fs, the incident ion is subjected to intense nuclear stopping. The kinetic energy decreases dramatically and starts to vibrate with great amplitude through successive collisions with lattice atoms and in the end the ion comes to rest in the bulk.

4. Conclusions

To study the interaction between low energy atomic carbons with tungsten surface, MD simulations were performed using a bond-order interatomic potential. Two types of surfaces, namely, bcc (001) and amorphous tungsten surfaces, are irradiated with the atomic carbons in the energy range from 0.5 eV to 200 eV at a fixed incidence angle ($\alpha = 0°$) and a substrate temperature (T = 300 K). Both particle and energy reflection coefficients increase with increasing the incident energy in the range from 0.5 eV to 10 eV and reach a maximum at 10 eV. Beyond 10 eV, the coeffi-

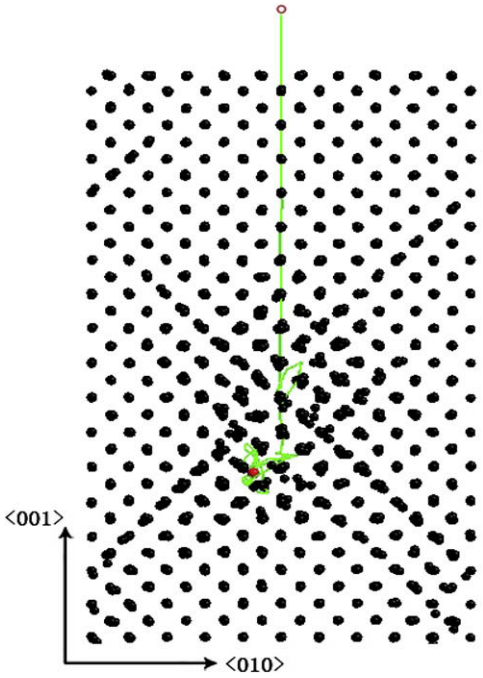

Fig. 4. The channeled trajectory of carbon atom at E_{in} = 150 eV in the tungsten bulk.

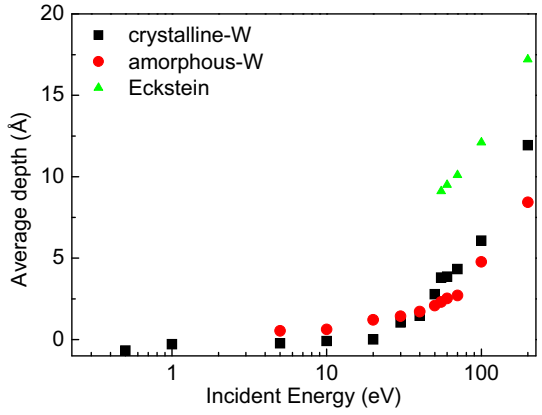

Fig. 3. Average depth (mean range) of atomic carbons implanted in crystalline tungsten at normal incidence on (001) tungsten surface and amorphous cell surface as a function of incident energy. The results calculated by Eckstein using TRIM.SP code [12] are also shown.

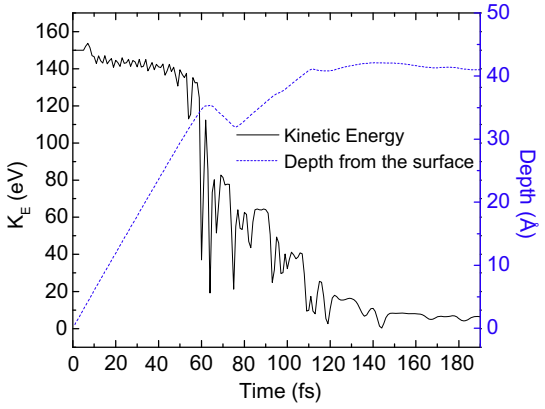

Fig. 5. Time variation of the kinetic energy of the channeled projectile in Fig. 4 as well as the projected range in tungsten bulk.

cients decrease monotonically with increasing the incident energy, in accordance with the results calculated by Eckstein using TRIM.SP code. Also discussed is the mean range of carbon with different incident energy on tungsten surface. In the low energy range below 10 eV, the un-scattered carbon atoms are absorbed on the top tungsten surface layer. With increasing the incident energy above 10 eV, the mean range increases and the range straggling also, attributed probably to the channeling effect.

Acknowledgements

This work was supported partially by the National Natural Science Foundation of China under Contract Nos. 10675130 and 10728510, the Knowledge Innovation Program of the Chinese Academy of Sciences, and the JSPS-CAS Core-University Program in the field of Plasma and Nuclear Fusion.

References

[1] A. Loarte, B. Lipschultz, A.S. Kukushkin, et al., Nucl. Fus. 47 (2007) S203.
[2] H. Bolt, V. Barabash, G. Federici, et al., J. Nucl. Mater. 307–311 (2002) 43.
[3] H. Bolt, V. Barabash, W. Krauss, et al., J. Nucl. Mater. 329–333 (2004) 66.
[4] G.-N. Luo, X.D. Zhang, D.M. Yao, X.Z. Gong, J.L. Chen, Z.S. Yang, Q. Li, B. Shi, J.G. Li, Phys. Scr. T128 (2007) 1.
[5] K. Krieger, H. Maier, R. Neu, et al., J. Nucl. Mater. 266–269 (1999) 207.
[6] J. Luthin, Ch. Linsmeier, Surf. Sci. 454–456 (2000) 78.
[7] W. Eckstein, J. Roth, Nucl. Instr. Meth. Phys. Res. B 53 (1991) 279.
[8] K. Schmid, J. Roth, W. Eckstein, J. Nucl. Mater. 290–293 (2001) 148.
[9] K. Schmid, J. Roth, J. Nucl. Mater. 302 (2002) 96.
[10] D. Naujoks, W. Eckstein, J. Nucl. Mater. 230 (1996) 93.
[11] N. Juslin, P. Erhart, P. Träskelin, et al., J. Appl. Phys. 98 (2005) 123520.
[12] W. Eckstein, Calculated Sputtering, Reflection and Range Values, IPP 9/132, 2002.
[13] W. Eckstein, J.P. Biersack, Appl. Phys. 34 (1984) 73.
[14] V. Rosato, G. Maino, A. Ventura, J. Phys.: Condens. Matter 1 (1989) 10021.